ACS OMEGA

http://pubs.acs.org/journal/acsodf

Article

Valine Supplementation Does Not Reduce Lipid Accumulation and Improve Insulin Sensitivity in Mice Fed High-Fat Diet

Qingquan Ma,*,§ Linlin Hu,§ Jialiang Zhu, Jiayi Chen, Zhishen Wang, Zhiyuan Yue, Minna Qiu, and Anshan Shan*

Cite This: *ACS Omega* 2020, 5, 30937−30945

Read Online

ACCESS | Metrics & More | Article Recommendations | Supporting Information

ABSTRACT: Branched-chain amino acids (BCAAs), particularly leucine, were reported to decrease obesity and relevant metabolic syndrome. However, whether valine has a similar effect has rarely been investigated. In the present study, mice were assigned into four treatments (n = 10): chow diet supplemented with water (CW) or valine (CV) and high-fat diet supplemented with water (HW) or valine (HV). Valine (3%, w/v) was supplied in the drinking water. The results showed that valine treatment markedly increased serum triglyceride and insulin levels of chow diet-fed mice. The body weight, serum triglyceride level, white adipose tissue weight, and glucose and insulin intolerance were significantly elevated by valine supplementation in high-fat diet-fed mice. Metabolomics and transcriptomics showed that several genes related to fat oxidation were downregulated, and arachidonic acid and linoleic acid metabolism were altered in the HV group compared to the HW group. In conclusion, valine supplementation did not suppress lipid deposition and metabolic disorders in mice, which provides a new understanding for BCAAs in the modulation of lipid metabolism.

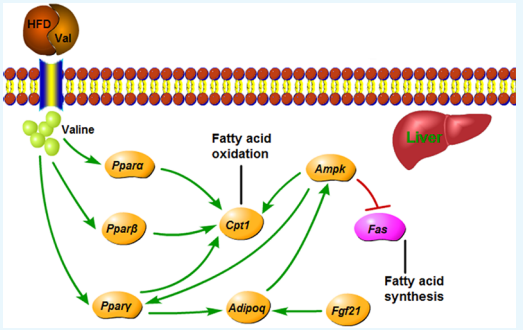

INTRODUCTION

Worldwide obesity has become a problem that cannot be ignored mainly as a consequence of changes in diet. It was estimated that there will be 2.16 billion adults overweight and 1.12 billion obese all over the globe by 2030.[1] Obesity is defined by WHO (World Health Organization) as an unusual accumulation of adipose tissue that presents a nutritional disorder and is associated with the occurrence of type 2 diabetes and insulin resistance. Therefore, attention has been focused on searching the supplements including macronutrients[2] that could effectively and safely treat or prevent obesity.[3]

Branched-chain amino acids (BCAAs), including leucine, isoleucine, and valine, account for around 35% of the essential amino acid requirements in mammals.[4] BCAAs are not only considered to be the building blocks of proteins but also play a regulatory role in lipid metabolism and fat deposition. Evidences showed that the addition of BCAAs significantly reduced fat deposition and controlled obesity. For instance, in a study where high-fat diet (HFD) was provided for six weeks and BCAAs were given for another two weeks, BCAAs treatment markedly reduced body weight and white adipose tissue (WAT) mass, as well as hepatic triglyceride (TG) concentration in mice.[5] Dietary supplementation with BCAAs also alleviated hepatic steatosis[6−8] and improved glucose homeostasis.[9,10] Besides the beneficial role for the mixture of BCAAs, individual BCAA supplementation showed a positive effect on suppressing fat accumulation and obesity. Long-term leucine treatment dramatically improved glycemic control in mouse models of obesity.[11] Similarly, it has reported that supplementation of leucine alleviates insulin resistance and liver steatosis in db/db mice.[12] Moreover, isoleucine prevented the accumulation of tissue triglycerides.[13] Our previous study revealed that leucine and isoleucine had the similar effect on reducing lipid accumulation and improving insulin sensitivity in obese mice fed HFD.[2] Nevertheless, little is known about the effect of another single BCAA valine on lipid metabolism and obesity. Although fat loss was stimulated in mice fed a valine-deprived diet for one week,[14] the impact of repletion of valine has not been reported. Therefore, we speculated that valine supplementation may inhibit fat accumulation.

In this study, we investigated the influence of valine supplementation on body weight, WAT weight, insulin sensitivity, and lipid profiles in mice. A combination of metabolomics and transcriptomics was employed to screen the possible metabolic pathways involved. Furthermore, real-time PCR was operated to confirm the results obtained by transcriptomics.

Received: August 3, 2020
Accepted: November 10, 2020
Published: November 24, 2020

https://dx.doi.org/10.1021/acsomega.0c03707
ACS Omega 2020, 5, 30937−30945

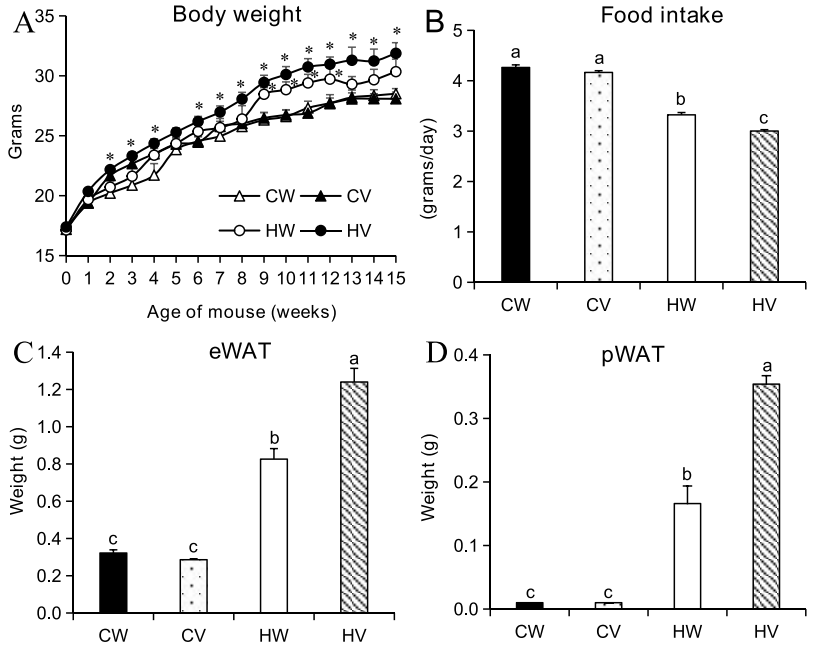

Figure 1. Effects of valine supplementation on body weight, food intake, and white adipose tissue weights in mice. (A) Body weight (grams); (B) food consumption (grams/day); (C) epididymal white adipose tissue (eWAT) (grams); and (D) perirenal white adipose tissue (pWAT) (grams). Values are means ± SEM (n = 10), and columns accompanied by the same letter are not significantly different from each other. *p < 0.05 vs CW. Abbreviations: chow diet + water (CW); chow diet + valine (CV); high-fat diet + water (HW); and high-fat diet + valine (HV).

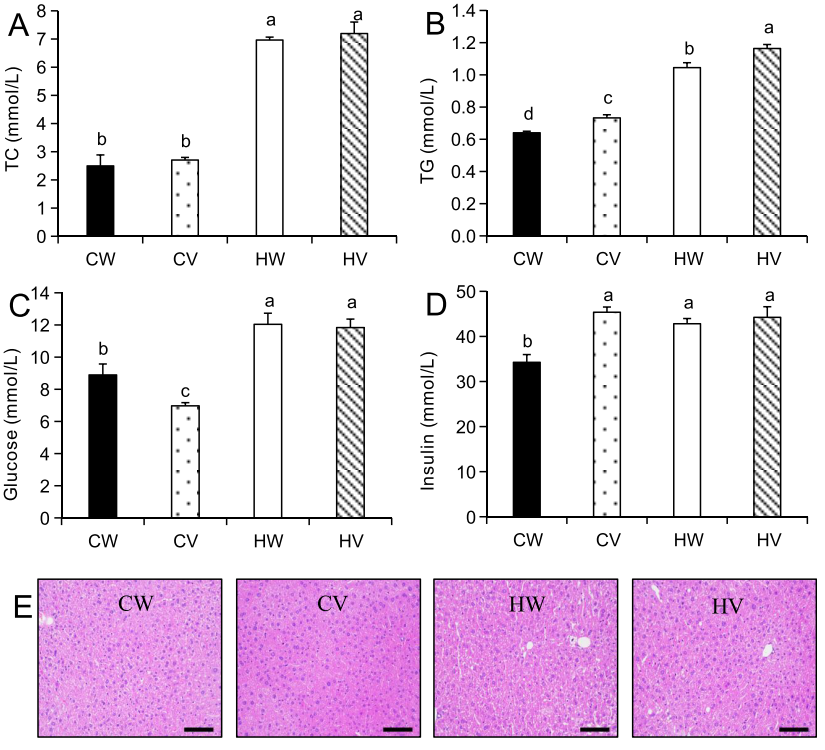

Figure 2. Effects of valine supplementation on serum biochemical parameters and hepatic histology in mice. (A) Total cholesterol (mmol/L); (B) total triglycerides (mmol/L); (C) glucose (mmol/L); and (D) insulin (mmol/L). Values are means ± SEM (n = 10), and columns accompanied by the same letter are not significantly different from each other. (E) Hepatic histological examination by H&E staining, scale bar = 100 μm. Abbreviations: chow diet + water (CW); chow diet + valine (CV); high-fat diet + water (HW); and high-fat diet + valine (HV).

RESULTS

Valine Supplementation Led to Increased Body Weight and Decreased Food Intake in HFD. As shown in Figure 1A, body weights of the four groups continuously grew. From the ninth week, the body weight of the HW group was higher compared with that of the CW group. Valine addition made no difference to body weight in mice fed chow diet, however, a tendency to gain body weight in mice fed HFD. The mice fed chow diet ingested more food than those fed HFD (Figure 1B), but HFD-fed mice took more energy than chow

https://dx.doi.org/10.1021/acsomega.0c03707
ACS Omega 2020, 5, 30937−30945

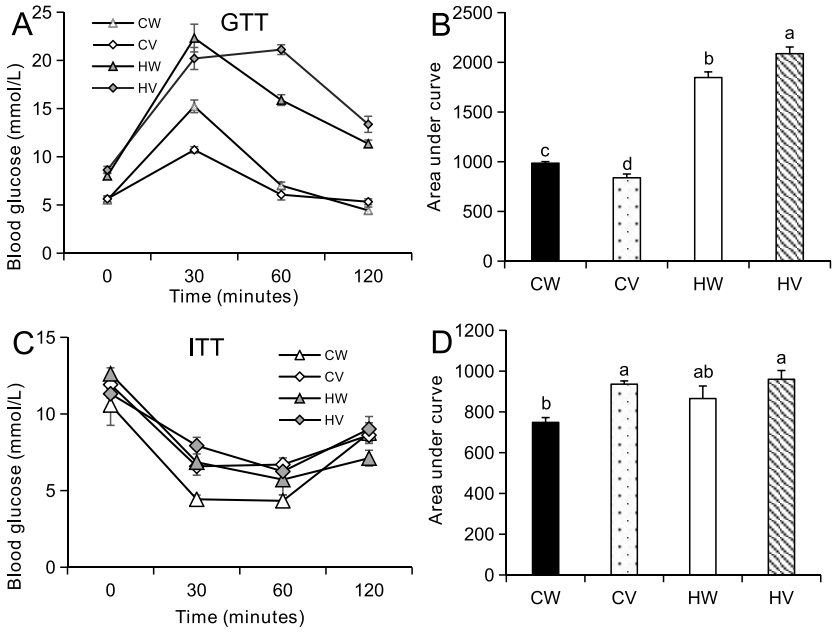

Figure 3. Effects of valine supplementation on glucose and insulin tolerance in mice. Glucose tolerance test (GTT) and insulin tolerance test (ITT) were performed at the 11th and 12th weeks of valine intervention. Before the GTT and ITT tests, the mice were fasted for 16 or 9 h, respectively. Glucose and insulin were intraperitoneally injected with a final concentration of 2 g/kg or 0.75 U/kg body weight. (A) Glucose tolerance test (GTT) and (B) corresponding area under curve (AUC). (C) Insulin tolerance test (ITT), and (D) corresponding AUC (n = 8/group). Values are means ± SEM (n = 8), and columns accompanied by the same letter are not significantly different from each other. Abbreviations: chow diet + water (CW); chow diet + valine (CV); high-fat diet + water (HW); and high-fat diet + valine (HV).

diet-fed mice due to higher energy density of HFD. Notably, valine addition decreased the food consumption and energy intake. The volumes of daily drinking water in CW, CV, HW, and HV were 3.49 ± 0.1, 3.51 ± 0.08, 3.55 ± 0.27, and 3.56 ± 0.13 mL, respectively. Therefore, the daily amounts of valine intake in CV and HV groups were 0.11 and 0.12 g. There was no significant difference in valine intake between CV and HV groups.

Valine Supplementation Caused Fat Accumulation and Increased Serum Triglycerides. As shown in Figure 1C,D, HFD significantly enlarged the volumes of epididymal white adipose tissue (eWAT) and perirenal white adipose tissue (pWAT) of mice in comparison to chow diet. Valine supplementation further increased the weights of eWAT and pWAT in the HV group. Serum total cholesterol and triglyceride concentrations were elevated in the HFD groups compared to chow diet groups (Figure 2A,B). Total cholesterol level was not altered, but serum triglyceride level was further upregulated by valine treatment in HFD- or chow diet-fed mice. The lipid amassed in the liver as vacuoles, which have an obvious appearance with hematoxylin and eosin (H&E) staining. Histological analysis showed that histomorphology was normal in chow-fed mice, but the increase of adipose hollow space and the disorder of hepatic plate arrangement were observed in both HFD-fed groups (Figure 2E).

Valine Supplementation Deteriorated Glucose and Insulin Tolerance. Fasting glucose and insulin concentrations in the CW group were markedly lower compared to the HW group (Figure 2C,D). Valine addition had no effect on fasting glucose and insulin in HFD-fed mice. However, valine supplementation increased fasting insulin and decreased fasting glucose under chow diet. For glucose tolerance test (GTT), the value of area under curve (AUC) in HFD was significantly larger than that in chow diet (Figure 3A,B). Valine supplementation improved glucose tolerance under chow diet but worsened glucose tolerance under HFD. For insulin tolerance test (ITT), valine treatment had no effect on AUC values of HFD-fed mice and deteriorated insulin tolerance under chow diet (Figure 3C,D).

Liver Metabolomics. To further explore the effect of valine treatment on the development of obesity in mice, metabolomics analysis was carried out between HW and HV groups. The ion peaks obtained from all experimental samples and quality control (QC) samples were Pareto-scaling processed to obtain a principal component analysis (PCA) model. QC samples in the PCA model were densely aggregated, suggesting that the result of this project was reproducible (Figure S1A). The orthogonal partial least squares discriminant analysis (OPLS-DA) score plot of HV was significantly different from that of HW in metabolism mode (Figure S1B). After sevenfold cross-validation, the model evaluation parameters R2Y and Q2 were 0.991 and 0.681, respectively, indicating that the model is steady and credible. The volcano plot intuitively showed the significant differences between the metabolites of two groups of samples (Figure S1C). Then, we performed hierarchical clustering of the 54 metabolites, and the heat map is presented in Figure 4. These metabolites showed significant differences in expression between HW and HV. A decrease in some amino acids can be observed in the HV group. Threefold increase was observed for hepatic valine level after valine treatment. By contrast, the levels of leucine, threonine, D-proline, methionine, serine, glycine, asparagine, phenylalanine, and tyrosine were decreased. Methyl donors, including betamine, dimethylglycine, glycerophosphocholine, 1-palmitoyl-*sn*-glycero-3-phosphocholine, cytidine 5′-diphosphocholine (CDP-choline), and lipid metabolites such as arachidonic acid and carnitine were downregulated.

The Kyoto Encyclopedia of Genes and Genomes (KEGG) pathway enrichment analysis (Figure 5) showed that important

https://dx.doi.org/10.1021/acsomega.0c03707
ACS Omega 2020, 5, 30937−30945

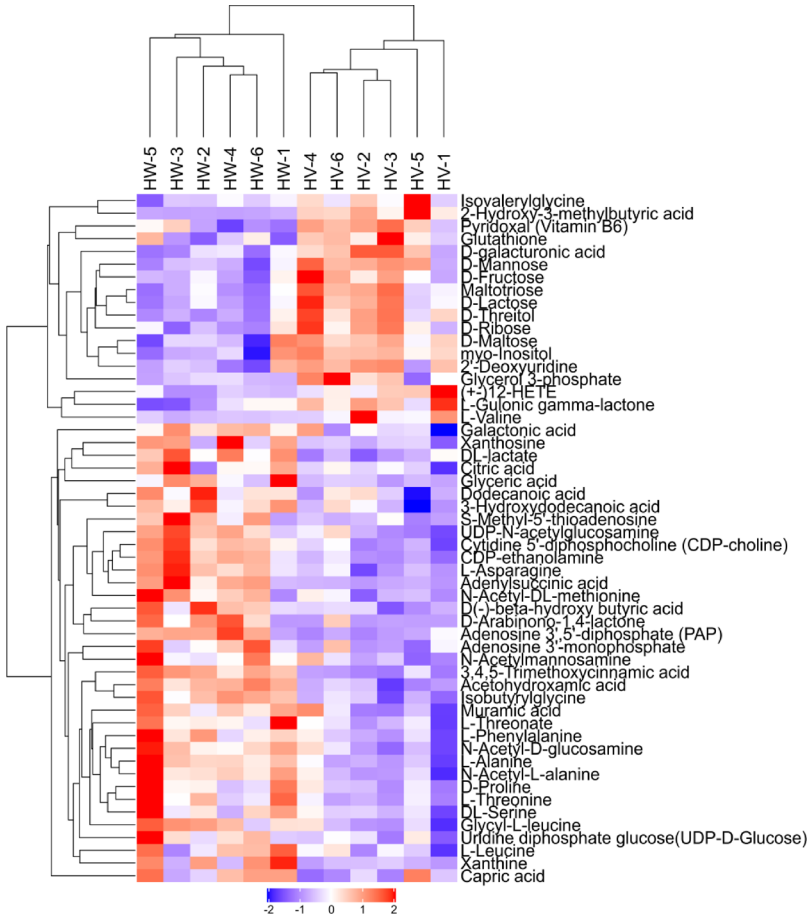

Figure 4. The hierarchical clustering of significant differences between metabolites for HV vs HW. Red indicates the upregulated metabolites in HV, and blue indicates the downregulated metabolites in HV. Scaled expression values are color-coded according to the legend on the bottom. Abbreviations: high-fat diet + valine (HV); and high-fat diet + water (HW).

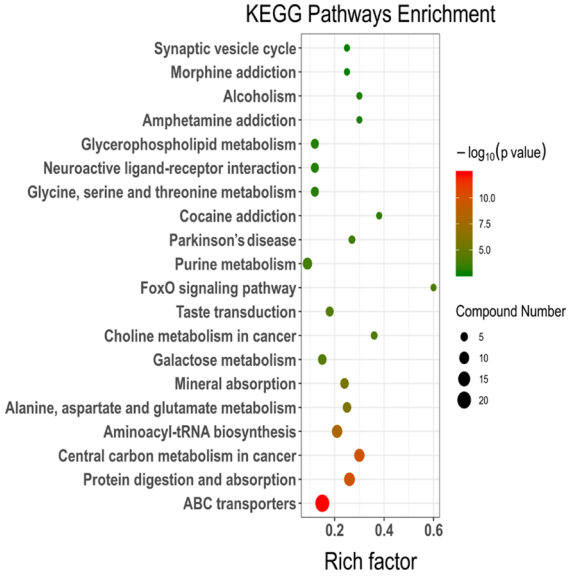

Figure 5. KEGG pathway enrichment results based on metabolite alteration. The size of the dots represents the number of significant metabolites; and the smaller *P* value indicates that KEGG pathway enrichment is more significant.

pathways such as ATP-binding cassette (ABC) transporters, protein digestion and absorption, central carbon metabolism in cancer, aminoacyl-tRNA biosynthesis, and alanine, aspartate, and glutamate metabolism were significantly altered.

Liver Transcriptomics. Volcano plot provided a quick look at the differences in gene expressions (Figure S2A). Some genes were upregulated but more genes were downregulated in the HV group compared to HW. In total, we analyzed 54 769 transcripts. Genes (352) were differentially expressed with 254 downregulated and 98 upregulated genes in the liver (Figure S2B). The top 30 enriched gene ontology (GO) terms are illustrated in Figure S3. Biological processes including epoxygenase P450 pathway and arachidonic acid metabolic process were highly enriched, and arachidonic acid activity was highly enriched in molecular functions. Several genes related to lipolysis, including peroxisome proliferator-activated receptor beta (*Pparβ*), carnitine palmitoyltransferase 1 (*Cpt1*), adiponectin, C1Q and collagen domain containing (*Adipoq*), and fibroblast growth factor 21 (*Fgf21*), were significantly downregulated in the HV group. Subsequent real-time PCR further validated the transcriptomics results. In addition, the HV group significantly decreased the mRNA expression of peroxisome proliferator-activated receptor alpha (*Pparα*), peroxisome proliferator-activated receptor gamma (*Pparγ*), and adenosine monophosphate-activated protein kinase (*Ampk*) and increased the mRNA expression of fatty acid synthase (*Fas*) compared with the HW group (Figure 6).

Combined Analysis of Metabolomics and Transcriptomics. All differentially expressed genes and metabolites were

https://dx.doi.org/10.1021/acsomega.0c03707
ACS Omega 2020, 5, 30937−30945

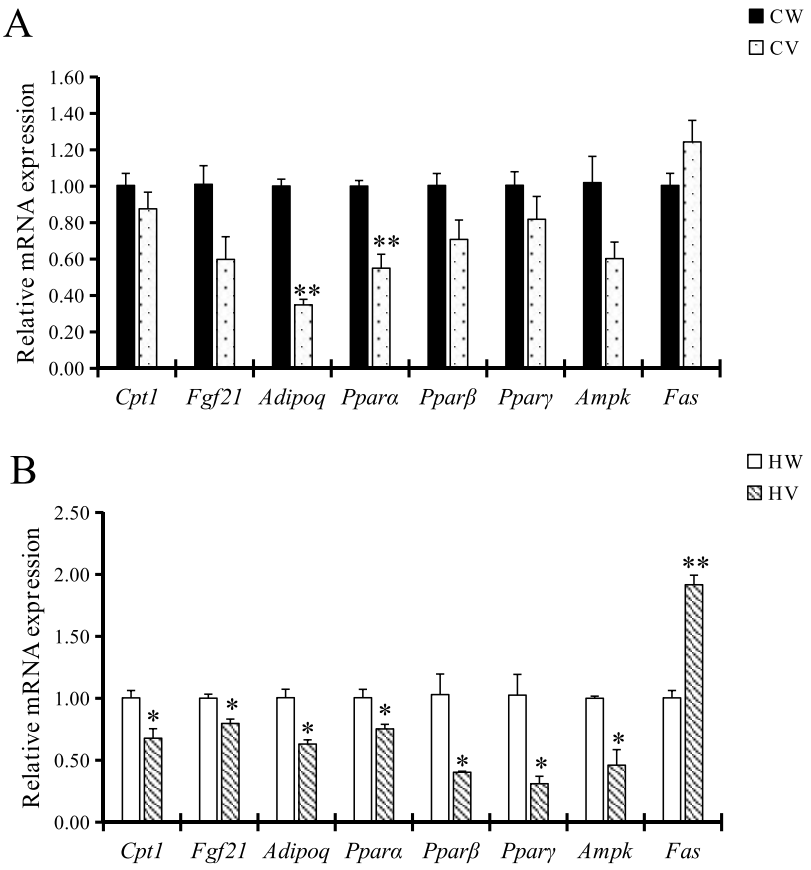

Figure 6. The liver mRNA expression of genes related to lipid metabolism. (A) Liver mRNA expression of *Cpt1*, *Fgf21*, *Adipoq*, *Pparα*, *Pparβ*, *Pparγ*, *Ampk*, and *Fas* in chow diet groups. *$p < 0.05$ vs CW and **$p < 0.01$ vs CW; (B) liver mRNA expression of *Cpt1*, *Fgf21*, *Adipoq*, *Pparα*, *Pparβ*, *Pparγ*, *Ampk*, and *Fas* in high-fat diet groups. *$p < 0.05$ vs HW and **$p < 0.01$ vs HW. Abbreviations: chow diet + water (CW); high-fat diet + water (HW); *Cpt1*: carnitine palmitoyltransferase 1; *Fgf21*: fibroblast growth factor 21; *Adipoq*: adiponectin, C1Q and collagen domain containing; *Pparα*: peroxisome proliferator-activated receptor alpha; *Pparβ*: peroxisome proliferator-activated receptor beta; *Pparγ*: peroxisome proliferator-activated receptor gamma; *Ampk*: adenosine monophosphate-activated protein kinase; and *Fas*: fatty acid synthase.

queried and mapped to pathways based on the online KEGG. Correlation analysis measures the degree of association between genes and metabolites. There were 52 marked pathways of gene expression, 104 significant pathways of metabolite expression, and the number of metabolic pathways involved in both omics was 10 (Figure S4A). The top 10 pathways with the highest number of genes and metabolites were statistically identified (Figure S4B). Lipid metabolism pathways such as arachidonic acid and linoleic acid metabolism are in the top five. Hierarchical clustering heat maps showed that both the differential genes and metabolites are clustered and may be in close step in biological processes (Figure S5).

DISCUSSION

In the context of continuous attention to BCAAs' antiobesity activity, we explored the effects of valine, a less well-studied BCAA, on lipid metabolism. The results showed that valine supplementation by drinking water aggravated fat deposition and increased serum triglyceride accompanied with worse glucose and insulin tolerance.

This is not the first report that BCAAs were invalid or even worsened toward fat accumulation. For example, in a study where BCAAs (109 mmol/L of each) or leucine (150 mmol/L) was supplemented in the drinking water for at least 14 weeks, body weight, body composition, insulin tolerance, and total cholesterol were not altered.[15] Notably, valine supplementation under HFD resulted in an increase in body weight and WAT weight but a decrease in energy intake, suggesting that valine participates in the repartition of lipid metabolism. There are two key factors that often influence the trend of the results: the diet energy percentage supplied by fat and the duration of nutrient treatment. For instance, BCAAs significantly reduced the body weight, WAT weight, and liver triglyceride content in mice fed diet containing 43% fat calories,[16] but has no effect in mice fed diet containing 60% fat calories.[15] Under the diet with similar fat supply, body weight and fat deposition were markedly reduced by leucine treatment for 14 weeks,[17] and in contrast, were increased by leucine supplementation for 24 weeks.[18] This suggests that there may be the threshold for both, beyond of which the use of valine is not beneficial for controlling the obesity. Furthermore, valine supplementation led to insulin resistance, which is consistent with the previous study about other amino acids.[19,20]

Metabolomic analysis revealed that the aggravation of obesity symptoms by valine supplementation is closely related to the abundance of polyunsaturated fatty acids (PUFA), the decrease of which has been observed in high-fat or high-sugar diet-fed animals.[21,22] Moreover, PUFA, especially arachidonic acid, was positively correlated with insulin sensitivity.[23] Insulin secretion was stimulated by arachidonic acid through the lipoxygenase pathway.[24]

https://dx.doi.org/10.1021/acsomega.0c03707
ACS Omega 2020, 5, 30937−30945

Transcriptional analysis screened a cluster of lipid metabolism-related genes that was responsible for promoting fat mass. *Pparβ* is a ligand-activated transcription factor related to the glycemic and lipid metabolism,[25] and activation of this factor could ameliorate hepatic steatosis by accelerating fatty acid oxidation.[26,27] *Pparβ* also upregulates the expression of *Cpt1*,[28] which is the rate-limiting enzyme in β-oxidation of long-chain fatty acid in hepatocyte. *Fgf21* is a metabolic regulator with broad effects on carbohydrate and lipid metabolism.[29] *Fgf21* could stimulate hepatic fatty acid oxidation, improve insulin resistance and steatosis in obese mice, and regulate liver glycogen synthesis and ketone body formation.[30−32] *Fgf21* activates the expression and secretion of adiponectin,[33] thereby regulating the balance of glycolipid metabolism and further improving the insulin sensitivity of the body. Adiponectin is a downstream effector of *Fgf21*. In obese mice with adiponectin knockout, the improvement effect of *Fgf21* on plasma triglycerides, liver steatosis, and liver injury disappeared.[33] Hence, it was speculated that valine supplementation caused the disorder of lipid metabolism by the downregulation of *Fgf21*-adiponectin axis.

A threefold increase of valine level could explain the decrease of leucine because BCAAs are transported by the same carrier. Previous studies found that additional dietary leucine reduced valine and isoleucine concentrations in serum and tissues.[34,35] One of the BCAAs at high concentrations could compete with the others via their common transport carriers.[36] Therefore, unbalanced BCAAs supply lead to antagonism of BCAAs,[37] which may explain the decrease of leucine. Our results observed the significant decrease of metabolites related with a methyl donor including betaine, dimethylglycine (the product of betaine metabolism), and glycerophosphocholine. In particular, betaine is not only a methyl donor and involved in the methionine cycle but also a lipotrope that inhibits hepatic fat deposition.[38] Inadequate dietary intake of methyl groups causes hypomethylation, which results in steatosis (fat deposition) and plasma dyslipidemia.[38] Higher serum betaine is associated with a more favorable lower body fat status.[39−41] Moreover, carnitine is a conditionally essential nutrient that allows mitochondrial import and oxidation of long chain fatty acids.[42] Carnitine deficiencies may occur due to certain disorders (such as liver disease).[43] It is assumed that the transport competition may inhibit the intestine absorption and transmembrane transport of betaine and choline by valine supplementation, ultimately leading to dyslipidemia.

In conclusion, valine supplementation for 15 weeks leads to increased fat deposition and decreased insulin sensitivity. The antagonism between leucine and valine may lead to adverse effects of valine supplementation. Therefore, the balance of BCAAs in dietary supply may act a dominated role in participating lipid homeostasis. Further experiments are needed to evaluate the influence of valine supplementation on lipid metabolism in already established mouse model.

MATERIALS AND METHODS

Experimental Animals and Diets. Six-week old C57BL/6 J male mice were purchased from HFK Biotechnology Co., Ltd. (Beijing, China). Mice were kept in a room at 23 °C on a 12:12 light−dark cycle. After a 7 d period of adaptation, the mice were randomly divided into four groups (n = 10): chow diet + water (CW), chow diet + valine (CV), high-fat diet (HFD) + water (HW), and HFD + valine (HV). Mice were caged separately with free access to water and food. Valine (3% (w/v) was supplemented in the drinking water. The valine solutions were made freshly each day. HFD provided 60% calories from fat (5.24 kcal/g, HFK Biotechnology Co., Ltd., Beijing, China). The dietary formula used in the experiment is shown in Table S3. Body weight and food intake were determined once a week. The study was approved by the Institutional Animal Care and Use Committee of Northeast Agricultural University.

Glucose and Insulin Tolerance Tests. GTT and ITT were tested at the 11th and 12th weeks of valine intervention. Before the GTT and ITT tests, the mice were fasted for 16 or 9 h, respectively. Glucose and insulin were injected intraperitoneally with a final concentration of 2 g/kg or 0.75 U/kg body weight. Blood was sampled from a tail vein, and glucose concentrations of mice were measured at 0, 30, 60, and 120 min after injection of glucose or insulin using a glucose meter (On Call, Hangzhou, China).

Sample Collection. At the 15th week of valine treatment, mice sank into a coma by inhaling ether after overnight fasting. Blood samples were collected from the eye pit and centrifuged at 3000 × g for 15 min. All mice were executed by cervical dislocation. The white adipose tissue and liver were quickly removed and weighed. Part of the tissues was stored in 4% paraformaldehyde for morphology analysis, and the rest was snap frozen in liquid nitrogen and stored at −80 °C until analysis.

Serum Parameter Determination. Serum glucose, total triglycerides, and total cholesterol were determined by enzymatic methods using commercial diagnostics kits (Biosino Biotechnology and Science Inc., Beijing, China). Insulin was determined using an enzyme-linked immunosorbent assay (ELISA) kit (Sangon Biotech Company, Shanghai, China).

Histological Analysis. Mouse liver tissue was embedded in paraffin and cut into 4 μm-thick slices. Histological morphology of slices was examined under a microscope after staining with hematoxylin and eosin.

Metabolomics. *Sample Preparation.* The liver homogenates were mixed with cold methanol/acetonitrile (1:1, v/v) by vortex for 60 s and ultrasonically processed twice and half an hour each time. The samples were centrifuged for 20 min (14 000 g, 4 °C). The samples were redissolved for liquid chromatography tandem−mass spectrometry (LC−MS) analysis.

LC−MS/MS Analysis. Analyses were performed using an ultrahigh performance liquid chromatography (UHPLC) system in Shanghai Applied Protein Technology Co., Ltd. Samples were separated using a hydrophilic interaction liquid chromatography (HILIC) column (Agilent 1290 Infinity). The column temperature was 25 °C, and the flow rate was 0.3 mL/min. The mobile phase consisted of A (25 mM ammonium acetate and 25 mM ammonium hydroxide in water) and B (acetonitrile). The gradient was 95% B for 0.5 min, was linearly declined to 65% in 7 min, was decreased to 40% in 1 min, kept for 1 min, then changed to 95% in 0.1 min, and kept for 3 min. During the whole process, the samples were placed in a 4 °C automatic sampler. After the sample detection, the first and second grade spectra of the sample were collected by a mass spectrometer (AB TripleTOF 6600). The ESI source conditions were set after separation of HILIC chromatography. The product ion scan is acquired using information dependent acquisition (IDA) with high sensitivity mode selected.

Data Handling. The original data is converted into .mzXML format by ProteoWizard, and XCMS program was used to perform peak alignment, retention time correction, and

https://dx.doi.org/10.1021/acsomega.0c03707
ACS Omega 2020, 5, 30937−30945

Table 1. Mice RT-PCR Primer Sequences[a]

gene	forward sequence (5′−3′)	reverse sequence (5′−3′)
β-Actin	CAGGCATTGCTGACAGGATG	TGCTGATCCACATCTGCTGG
Cpt1	CCCAGTCAGATTCCAACC	TCACCAAAATGACCTAGCC
Fgf21	GCTGGAGGACGGTTACAA	GTCAGAGGAGCCCACATC
Adipoq	GGCCACTTTCTCCTCATTT	GTAACGTCATCTTCGGCAT
Pparα	CATTTCTCCTTGGCGTGT	CCTCAGACCTTGCTTTGG
Pparβ	CCACGAGTTCTTGCGAAGT	GATGAAGAGCGCCAGGTC
Pparγ	CGAGAAGGAGAAGCTGTTG	TCAGCGGGAAGGACTTTA
Ampk	CTACCTAGCAACCAGCCCAC	ACGTCTGAGGGCTTTCCTTG
Fas	TGCTTGCTGGCTCACAGTTA	ATCAGTTTCACGAACCCGCC

[a]Abbreviations: *Cpt1*: carnitine palmitoyltransferase 1; *Fgf21*: fibroblast growth factor 21; *Adipoq*: adiponectin, C1Q and collagen domain containing; *Pparα*: peroxisome proliferator-activated receptor alpha; *Pparβ*: peroxisome proliferator-activated receptor beta; *Pparγ*: peroxisome proliferator-activated receptor gamma; *Ampk*: adenosine monophosphate-activated protein kinase; and *Fas*: fatty acid synthase.

extraction of peak area. Structure identification of metabolites was carried out by the method of matching accuracy m/z value (<25 ppm) and MS/MS spectra and searched by an in-house database.

Transcriptomics. RNA quantification and qualification: RNA degradation and contamination was examined by 1% agarose gel electrophoresis. RNA purity (OD260/280), concentration, and absorption peak of nucleic acid were detected using Nanodrop. RNA integrity and concentration were measured accurately using an Agilent 2100 RNA Nano 6000 Assay Kit (Agilent Technologies, CA, USA).

Library construction and quality control: a total amount of 3 μg RNA per sample was used as an input material for the RNA sample preparations. mRNA of eukaryon was enriched using magnetic beads with oligo. Adding fragmentation buffer broke randomly mRNA. First-strand cDNA was synthesized using random hexamer. Second-strand cDNA synthesis was synthesized using buffer, dNTPs, RNase H, and DNA polymerase I. Then, cDNA was purified by AMPure XP beads.[44] The purified double-stranded cDNA was performed by terminal repair, with adding A tail and connecting the sequencing connector, and then the fragment size was selected with AMPure XP beads. Finally, cDNA libraries were obtained via PCR enrichment. The library was initially quantified using Qubit 2.0, diluted to 1 ng/μL, and then insert size was detected using Agilent 2100. At last, library quality was assessed using an Agilent Bioanalyzer 2100 system.

Quantitative Real-Time PCR. Total liver RNA was extracted using Trizol reagent (Ambion). The purity and concentration of RNA were assessed by absorbance at 260/280 nm before cDNA synthesis. For reverse transcription, 1 μg of mRNA was converted to first-strand complementary DNA in 20 μL reactions using a PrimeScript RT reagent Kit with gDNA Eraser (TaKaRa, Dalian, China). Relative gene expression levels were determined using real-time PCR detection system with TB Green Premix Ex Taq (TaKaRa, Dalian, China). Calculations were made by method of $2^{-\Delta\Delta Ct}$ using β-actin as an internal control. Primer sequences used are listed in Table 1.

Treatment of Animals. The agreement used in the study was approved by the Northeast Agricultural University Institutional Animal Care and Use Committee, and the ethical treatment of animals used in this experiment complied with the Animal Welfare Committee protocol (#NEAU-[2013]-9) in Northeast Agricultural University.

Statistical Analysis. All the data were expressed as mean ± SEM. One-way analysis of variance (ANOVA) was conducted to evaluate the significance of differences between the means of groups. Duncan's post hoc test was used for multiple group comparisons. In all analyses, $p < 0.05$ was considered significant. The analysis was performed using SPSS Statistics (Chicago, USA).

■ ASSOCIATED CONTENT

Supporting Information

The Supporting Information is available free of charge at https://pubs.acs.org/doi/10.1021/acsomega.0c03707.

PCA, OPLS-DA score plot, and volcano plot for the metabolic profiling results of liver tissue for HV vs HW (Figure S1); volcano plot and hierarchical clustering of differential genes for HV vs HW (Figure S2); gene ontology (GO) enrichment histogram of differential genes (Figure S3); Venn of differential genes and differential metabolites involved in pathways and the top 10 pathways with the highest number of genes and metabolites involved (Figure S4); correlation analysis Spearman differential genes and differential metabolites (Figure S5); summary of significantly different metabolites between HV and HW based on OPLS-DA VIP (variable importance for the projection) more than one (Table S1); summary of significantly different genes between HV and HW by transcriptomics (Table S2) (PDF)

■ AUTHOR INFORMATION

Corresponding Authors

Qingquan Ma − *Institute of Animal Nutrition, Northeast Agricultural University, Harbin 150030, China*; Email: maqingquan@neau.edu.cn

Anshan Shan − *Institute of Animal Nutrition, Northeast Agricultural University, Harbin 150030, China*; orcid.org/0000-0003-2667-8912; Phone: +86 451 55190685; Email: asshan@neau.edu.cn; Fax: +86 451 55103336

Authors

Linlin Hu − *Institute of Animal Nutrition, Northeast Agricultural University, Harbin 150030, China*

Jialiang Zhu − *Institute of Animal Nutrition, Northeast Agricultural University, Harbin 150030, China*

Jiayi Chen − *Institute of Animal Nutrition, Northeast Agricultural University, Harbin 150030, China*

Zhishen Wang − *Institute of Animal Nutrition, Northeast Agricultural University, Harbin 150030, China*

Zhiyuan Yue − *Institute of Animal Nutrition, Northeast Agricultural University, Harbin 150030, China*

https://dx.doi.org/10.1021/acsomega.0c03707
ACS Omega 2020, 5, 30937−30945

Minna Qiu − *Institute of Animal Nutrition, Northeast Agricultural University, Harbin 150030, China*

Complete contact information is available at: https://pubs.acs.org/10.1021/acsomega.0c03707

Author Contributions

[§]Q.M. and L.H. contributed equally to this manuscript.

Notes

The authors declare no competing financial interest.

■ ACKNOWLEDGMENTS

This work was supported by grants from the National Key Research and Development Project (2018YFD0501202), the National Natural Science Foundation of China (31772611), and the Research and Development of Scientific and Technological Achievements in Heilongjiang Province College (2018-0177).

■ ABBREVIATIONS

BCAAs, branched-chain amino acids; CW, chow diet + water; CV, chow diet + valine; HW, high-fat diet + water; HV, high-fat diet + valine; *Pparβ*, peroxisome proliferator-activated receptor beta; *Cpt1*, carnitine palmitoyltransferase 1; *Adipoq*, adiponectin, C1Q and collagen domain containing; *Fgf21*, fibroblast growth factor 21; WHO, world health organization; HFD, high-fat diet; WAT, white adipose tissue; TG, triglyceride; eWAT, epididymal white adipose tissue; pWAT, perirenal white adipose tissue; H&E, hematoxylin and eosin; GTT, glucose tolerance test; AUC, area under curve; ITT, insulin tolerance test; QC, quality control; PCA, principal component analysis; OPLS-DA, orthogonal partial least squares discriminant analysis; ABC, ATP-binding cassette; KEGG, Kyoto Encyclopedia of Genes and Genomes; GO, gene ontology; *Pparα*, peroxisome proliferator-activated receptor alpha; *Pparγ*, peroxisome proliferator-activated receptor gamma; *Ampk*, adenosine monophosphate-activated protein kinase; *Fas*, fatty acid synthase; PUFA, polyunsaturated fatty acids; LC−MS, liquid chromatography tandem-mass spectrometry; ISVF, ionspray voltage floating; IDA, information dependent acquisition; CE, collision energy; DP, declustering potential

■ REFERENCES

(1) Popkin, B. M.; Adair, L. S.; Ng, S. W. NOW AND THEN: The global nutrition transition: The pandemic of obesity in developing countries. *Nutr. Rev.* **2012**, *70*, 3−21.

(2) Ma, Q.; Zhou, X.; Hu, L.; Chen, J.; Zhu, J.; Shan, A. Leucine and isoleucine have similar effects on reducing lipid accumulation, improving insulin sensitivity and increasing the browning of WAT in high-fat diet-induced obese mice. *Food Funct.* **2020**, *11*, 2279−2290.

(3) Ma, Q.; Zhou, X.; Sun, Y.; Hu, L.; Zhu, J.; Shao, C.; Meng, Q.; Shan, A. Threonine, but not lysine and methionine, reduces fat accumulation by regulating lipid metabolism in obese mice. *J. Agric. Food Chem.* **2020**, *68*, 4876−4883.

(4) Harper, A. E.; Miller, R. H.; Block, K. P. Branched-chain amino acid metabolism. *Annu. Rev. Nutr.* **1984**, *4*, 409−454.

(5) Arakawa, M.; Masaki, T.; Nishimura, J.; Seike, M.; Yoshimatsu, H. The effects of branched-chain amino acid granules on the accumulation of tissue triglycerides and uncoupling proteins in diet-induced obese mice. *Endocr. J.* **2011**, *58*, 161−170.

(6) Yang, Z.; Huang, S.; Zou, D.; Dong, D.; He, X.; Liu, N.; Liu, W.; Huang, L. Metabolic shifts and structural changes in the gut microbiota upon branched-chain amino acid supplementation in middle-aged mice. *Amino Acids* **2016**, *48*, 2731−2745.

(7) Shimomura, Y.; Murakami, T.; Nakai, N.; Nagasaki, M.; Harris, R. A. Exercise promotes BCAA catabolism: Effects of BCAA supplementation on skeletal muscle during exercise. *J. Nutr.* **2004**, *134*, 1583S−1587S.

(8) Honda, T.; Ishigami, M.; Luo, F.; Lingyun, M.; Ishizu, Y.; Kuzuya, T.; Hayashi, K.; Nakano, I.; Ishikawa, T.; Feng, G.-G.; Katano, Y.; Kohama, T.; Kitaura, Y.; Shimomura, Y.; Goto, H.; Hirooka, Y. Branched-chain amino acids alleviate hepatic steatosis and liver injury in choline-deficient high-fat diet induced NASH mice. *Metab., Clin. Exp.* **2017**, *69*, 177−187.

(9) Miyake, T.; Abe, M.; Furukawa, S.; Tokumoto, Y.; Toshimitsu, K.; Ueda, T.; Yamamoto, S.; Hirooka, M.; Kumagi, T.; Hiasa, Y.; Matsuura, B.; Onji, M. Long-term branched-chain amino acid supplementation improves glucose tolerance in patients with nonalcoholic steatohepatitis-related cirrhosis. *Intern. Med.* **2012**, *51*, 2151−2155.

(10) Nishitani, S.; Takehana, K.; Fujitani, S.; Sonaka, I. Branched-chain amino acids improve glucose metabolism in rats with liver cirrhosis. *Am. J. Physiol.: Gastrointest. Liver Physiol.* **2005**, *288*, G1292−G1300.

(11) Guo, K.; Yu, Y. H.; Hou, J.; Zhang, Y. Chronic leucine supplementation improves glycemic control in etiologically distinct mouse models of obesity and diabetes mellitus. *Nutr. Metab.* **2010**, *7*, 57−66.

(12) Chen, K.-H.; Chen, Y.-L.; Tang, H.-Y.; Hung, C.-C.; Yen, T.-H.; Cheng, M.-L.; Shiao, M.-S.; Chen, J.-K. Dietary leucine supplement ameliorates hepatic steatosis and diabetic nephropathy in db/db Mice. *Int. J. Mol. Sci.* **2018**, *19*, 1921.

(13) Nishimura, J.; Masaki, T.; Arakawa, M.; Seike, M.; Yoshimatsu, H. Isoleucine prevents the accumulation of tissue triglycerides and upregulates the expression of PPARα and uncoupling protein in diet-induced obese mice. *J. Nutr.* **2010**, *140*, 496−500.

(14) Du, Y.; Meng, Q.; Zhang, Q.; Guo, F. Isoleucine or valine deprivation stimulates fat loss via increasing energy expenditure and regulating lipid metabolism in WAT. *Amino Acids* **2012**, *43*, 725−734.

(15) Nairizi, A.; She, P.; Vary, T. C.; Lynch, C. J. Leucine supplementation of drinking water does not alter susceptibility to diet-induced obesity in mice. *J. Nutr.* **2009**, *139*, 715−719.

(16) Freudenberg, A.; Petzke, K. J.; Klaus, S. Dietary L-leucine and L-alanine supplementation have similar acute effects in the prevention of high-fat diet-induced obesity. *Amino Acids* **2013**, *44*, 519−528.

(17) Zhang, Y.; Guo, K.; Leblanc, R. E.; Loh, D.; Schwartz, G. J.; Yu, Y.-H. Increasing dietary leucine intake reduces diet-induced obesity and improves glucose and cholesterol metabolism in mice via multimechanisms. *Diabetes* **2007**, *56*, 1647−1654.

(18) Li, X.; Wang, X.; Liu, R.; Ma, Y.; Guo, H.; Hao, L.; Yao, P.; Liu, L.; Sun, X.; He, K.; Cao, W.; Yang, X. Chronic leucine supplementation increases body weight and insulin sensitivity in rats on high-fat diet likely by promoting insulin signaling in insulin-target tissues. *Mol. Nutr. Food Res.* **2013**, *57*, 1067−1079.

(19) Um, S. H.; D'Alessio, D.; Thomas, G. Nutrient overload, insulin resistance, and ribosomal protein S6 kinase 1, S6K1. *Cell Metab.* **2006**, *3*, 393−402.

(20) Tremblay, F.; Lavigne, C.; Jacques, H.; Marette, A. Role of dietary proteins and amino acids in the pathogenesis of insulin resistance. *Annu. Rev. Nutr.* **2007**, *27*, 293−310.

(21) Fukuchi, S.; Hamaguchi, K.; Seike, M.; Himeno, K.; Sakata, T.; Yoshimatsu, H. Role of fatty acid composition in development of metabolic disorders in sucrose induces obese rats. *Exp. Biol. Med.* **2004**, *229*, 486−493.

(22) Buettner, R.; Parhofer, K. G.; Woenckhaus, M.; Wrede, C. E.; Kunz-Schughart, L. A.; Schölmerich, J.; Bollheimer, L. C. Defining high-fat-diet rat models: metabolic and molecular effects of different fat types. *J. Mol. Endocrinol.* **2006**, *36*, 485−501.

(23) Storlien, L. H.; Baur, L. A.; Kriketos, A. D.; Pan, D. A.; Cooney, G. J.; Jenkins, A. B.; Calvert, G. D.; Campbell, L. V. Dietary fats and insulin action. *Diabetologia* **1996**, *39*, 621−631.

(24) Ahrén, B.; Magrum, L. J.; Havel, P. J.; Greene, S. F.; Phinney, S. D.; Johnson, P. R.; Stern, J. S. Augmented insulinotropic action of arachidonic acid through the lipoxygenase pathway in the obese zucker rat. *Obes. Res.* **2000**, *8*, 475−480.

(25) Vázquez-Carrera, M. Unraveling the effects of PPARβ/δ on insulin resistance and cardiovascular disease. *Trends Endocrinol. Metab.* **2016**, *27*, 319−334.
(26) Bojic, L. A.; Telford, D. E.; Fullerton, M. D.; Ford, R. J.; Sutherland, B. G.; Edwards, J. Y.; Sawyez, C. G.; Gros, R.; Kemp, B. E.; Steinberg, G. R.; Huff, M. W. PPARδ activation attenuates hepatic steatosis in *Ldlr*−/− mice by enhanced fat oxidation, reduced lipogenesis, and improved insulin sensitivity. *J. Lipid Res.* **2014**, *55*, 1254−1266.
(27) Wu, H.-T.; Chen, C.-T.; Cheng, K.-C.; Li, Y.-X.; Yeh, C.-H.; Cheng, J.-T. Pharmacological activation of peroxisome proliferator-activated receptor δ improves insulin resistance and hepatic steatosis in high fat diet-induced diabetic mice. *Horm. Metab. Res.* **2011**, *43*, 631−635.
(28) Wan, J.; Jiang, L.; Lü, Q.; Ke, L.; Li, X.; Tong, N. Activation of PPARdelta up-regulates fatty acid oxidation and energy uncoupling genes of mitochondria and reduces palmitate-induced apoptosis in pancreatic beta-cells. *Biochem. Biophys. Res. Commun.* **2010**, *391*, 1567−1572.
(29) Potthoff, M. J.; Kliewer, S. A.; Mangelsdorf, D. J. Endocrine fibroblast growth factors 15/19 and 21: from feast to famine. *Genes Dev.* **2012**, *26*, 312−324.
(30) Coskun, T.; Bina, H. A.; Schneider, M. A.; Dunbar, J. D.; Hu, C. C.; Chen, Y.; Moller, D. E.; Kharitonenkov, A. Fibroblast growth factor 21 corrects obesity in mice. *Endocrinology* **2008**, *149*, 6018−6027.
(31) Badman, M. K.; Pissios, P.; Kennedy, A. R.; Koukos, G.; Flier, J. S.; Maratos-Flier, E. Hepatic fibroblast growth factor 21 is regulated by PPARα and is a key mediator of hepatic lipid metabolism in ketotic states. *Cell Metab.* **2007**, *5*, 426−437.
(32) Inagaki, T.; Dutchak, P.; Zhao, G.; Ding, X.; Gautron, L.; Parameswara, V.; Li, Y.; Goetz, R.; Mohammadi, M.; Esser, V.; Elmquist, J. K.; Gerard, R. D.; Burgess, S. C.; Hammer, R. E.; Mangelsdorf, D. J.; Kliewer, S. A. Endocrine regulation of the fasting response by PPARα-mediated induction of fibroblast growth factor 21. *Cell Metab.* **2007**, *5*, 415−425.
(33) Lin, Z.; Tian, H.; Lam, K. S. L.; Lin, S.; Hoo, R. C. L.; Konishi, M.; Itoh, N.; Wang, Y.; Bornstein, S. R.; Xu, A.; Li, X. Adiponectin mediates the metabolic effects of FGF21 on glucose homeostasis and insulin sensitivity in mice. *Cell Metab.* **2013**, *17*, 779−789.
(34) Tannous, R. I.; Rogers, Q. R.; Harper, A. E. Effect of leucine—isoleucine antagonism on the amino acid pattern of plasma and tissues of the rat. *Arch. Biochem. Biophys.* **1966**, *113*, 356−361.
(35) Clark, A. J.; Yamada, C.; Swendseid, M. E. Effect of L-leucine on amino acid levels in plasma and tissue of normal and diabetic rats. *Am. J. Physiol.* **1968**, *215*, 1324−1328.
(36) Shotwell, M. A.; Kilberg, M. S.; Oxender, D. L. The regulation of neutral amino acid transport in mammalian cells. *Biochim. Biophys. Acta* **1983**, *737*, 267−284.
(37) Olde Damink, S. W. M.; Dejong, C. H. C.; Deutz, N. E. P.; van Berlo, C. L. H.; Soeters, P. B. Upper gastrointestinal bleeding: an ammoniagenic and catabolic event due to the total absence of isoleucine in the haemoglobin molecule. *Med. Hypotheses* **1999**, *52*, 515−519.
(38) Craig, S. A. S. Betaine in human nutrition. *Am. J. Clin. Nutr.* **2004**, *80*, 539−549.
(39) Chen, Y.-M.; Liu, Y.; Liu, Y.-H.; Wang, X.; Guan, K.; Zhu, H.-L. Higher serum concentrations of betaine rather than choline is associated with better profiles of DXA-derived body fat and fat distribution in Chinese adults. *Int. J. Obes.* **2015**, *39*, 465−471.
(40) Gao, X.; Randell, E.; Zhou, H.; Sun, G. Higher serum choline and betaine levels are associated with better body composition in male but not female population. *PLoS One* **2018**, *13*, No. e0193114.
(41) Gao, X.; Wang, Y.; Randell, E.; Pedram, P.; Yi, Y.; Gulliver, W.; Sun, G. Higher dietary choline and betaine intakes are associated with better body composition in the adult population of newfoundland. *PLoS One* **2016**, *11*, No. e0155403.
(42) Noland, R. C.; Koves, T. R.; Seiler, S. E.; Lum, H.; Lust, R. M.; Ilkayeva, O.; Stevens, R. D.; Hegardt, F. G.; Muoio, D. M. Carnitine insufficiency caused by aging and overnutrition compromises mitochondrial performance and metabolic control*. *J. Biol. Chem.* **2009**, *284*, 22840−22852.
(43) Flanagan, J. L.; Simmons, P. A.; Vehige, J.; Willcox, M. D.; Garrett, Q. Role of carnitine in disease. *Nutr. Metab.* **2010**, *7*, 30−43.
(44) Dong, N.; Li, X.; Xue, C.; Zhang, L.; Wang, C.; Xu, X.; Shan, A. Astragalus polysaccharides alleviates LPS - induced inflammation via the NF - κB/MAPK signaling pathway. *J. Cell. Physiol.* **2020**, *235*, 5525−5540.

https://dx.doi.org/10.1021/acsomega.0c03707
ACS Omega 2020, 5, 30937−30945